GOSPODARKA SUROWCAMI MINERALNYMI – MINERAL RESOURCES MANAGEMENT

2022 Volume 38 Issue 4 Pages 231–255

DOI: 10.24425/gsm.2022.143623

T. MARIS MURUGAN[1], R. KIRUBA SHANKAR[2]

The implementation of a coefficient diagram method based polynomial controller for a non-linear process with a distributed control system in a chlorine scrubber system

Introduction

In recent years, saltwater desalination has appeared to offer a solution to the problem of water scarcity; it is an environmentally friendly method of producing purified water. Fresh water makes up less than 0.5 percent of the total water supply on the planet. Massive Fresh water reservoirs exist beneath the earth, and much of it is at too deep a level to reach, but it can be accessed cost-effectively. The capacity and use of salt water reverse osmosis (SWRO) desalination technology is rapidly expanding around the world, and several countries in South Asia, North Africa, and the Arabian Peninsula have already turned to seawater desalination to improve their water supply (Tlili et al. 2003). A desalination process is a method

✉ Corresponding Author: T. Maris Murugan; e-mail: marismurugare@gmail.com

[1] Erode Sengunthar Engineering College, Department of Electronics and Instrumentation Engineering, Perundurai, Erode, Tamil Nadu, 638 057, India; ORCID iD: 0000-0001-5721-1739; e-mail: marismurugare@gmail.com

[2] KPR Institute of Engineering and Technology, Department of Electronics and Communication Engineering, Coimbatore, Tamil Nadu, 641 407, India; e-mail: kirubas12@gmail.com

of producing purified water through the removal of excess minerals, salts, and other contaminants from sea water (see Figure 1). Two common distillation processes used for desalination across the world are membrane distillation and thermal distillation. Thermal distillation methods are frequently employed in the Middle East. In the United States, membrane distillation methods are generally employed. These systems treat the feed water by forcing it through membranes using a pressure differential (Hamamci et al. 2006).

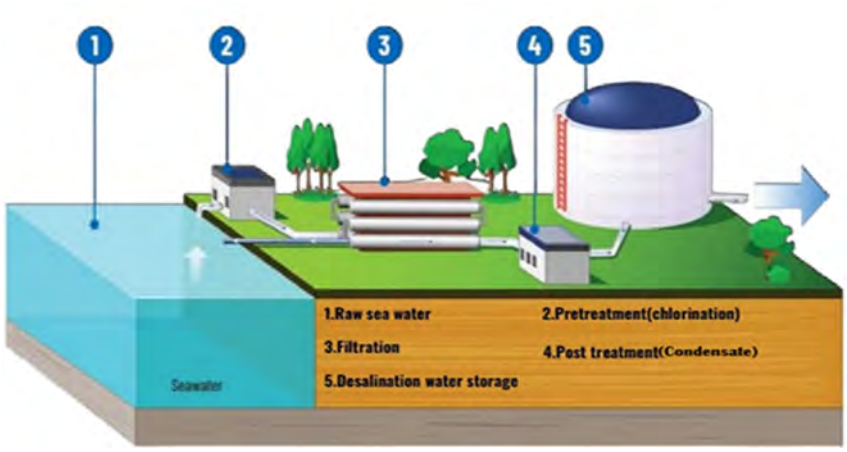

Fig. 1. Saline water desalination process

Rys. 1. Proces odsalania wody zasolonej

The first stage in a desalination plant is to separate microorganisms from seawater using chlorine gas. Chlorination is performed by the use of either gaseous chlorine from cylinders or in-situ electrogenerated sodium hypochlorite. To prevent marine life (mussels, barnacles, and tiny fish, for example) from entering the intake system, saltwater is frequently chlorinated at the seawater intake. Chlorine will begin to flow from the scrubber as soon as the solution is saturated with chlorine. Because chlorine is a hazardous irritant to people, the emergency chlorine gas scrubber system is used to safely neutralize unplanned chlorine leaks in the chlorine storage area. In the event of a chlorine release, an alert is activated, employees are relocated away from the site for a certain period, and dampers are manually opened. This results in unsafe working conditions and wastes time. The whole chlorination plant's instrumentation and control are automated. Many researchers have recently developed various control strategies to control the chlorination plant.

Graphene oxide (GO) has been used to improve membrane characteristics for distillation in a variety of methods, including the creation of free-standing GO membranes, GO-surface altered vesicles, and cast vesicles (Hegab and Zou 2015). To evaluate the potential of desalination as a viable alternative water supply for China by examining the economics of saltwater (Zhou and Tol 2004). Improved desalination technologies and accumulated managerial

experience have contributed to a significant reduction in the unit price of water over time. A decarbonization reactor is used to investigate the pre-treatment of geothermal fluids destined for desalination by reverse osmosis (RO) at the Gabbs (Tunisia) plant. The softness of the waters is accomplished by planting calcium carbonate ingredients obtained on-site in an open double-partition reactor while the air is bubbling.

Particle swarm optimization (PSO) and genetic algorithms (GA) have been proposed for the conical tank's four operating parts each having a 7 cm height. For a given area, a first-order plus dead time (FOPDT) model of the conical tank method performance, robustness, and energy (George et al. 2020).

A non-contact water salinity sensor was proposed to detect the salinity of previously processed saltwater desalination water (Sonehara et al. 2016). The Davison methodology, as well as the Tanttu and Liestehto methods, are used to tune centralized proportional and integral (PI) controllers. Findings: using a centralized PI controller to reduce the interaction between the two interacting conical tanks increases flexibility (Manic et al. 2016). To adjust for process changes and to keep the liquid level on target, the internal model controller (IMC), proportional-integral and derivative (PID), and IMC-PID were used (Lavanya et al. 2013). CDM is an important category in the algebraic approach. Level management is critical in most chemical facilities because optimum production ratios and stocks are attained by proper flow and the control of levels in chemical reactions (Bhaba and Somasundaram 2009; Kumpanya et al. 2000). The CDM concept is used to simplify the design of a PI controller for a higher-order plant. It is utilized to manage the speed of the two-inertia system. Despite its simplicity in design, CDM has reduced speed as well as torsional resonance (Kanagasabai et al. 2014; Coelho et al. 2017). The controller used has a ZN-based PID controller as well as an IMC based PID controller (Imal 2009; Roengruen et al. 2009).

An intelligent hybrid of the decentralized coefficient diagram method (CDM) technique and an invention of the LFC (load frequency control) method based on an optimum design of the CDM controller is employed in a thermal power plant (Heshmati et al. 2020). The DCM controller uses a combined servo state-feedback mechanism to regulate the aircraft's longitudinal and lateral movements (Asa et al. 2021). Artificial intelligence approaches, such as fuzzy inference systems, are utilized to increase the consistency and resilience of decision-making in drinking-water-treatment-plant (DWTP) facilities. Also created was an enhanced control system for selecting the mixed dosage of ClO_2 and NaOCl during the main disinfection stage of a large-scale DWTP (Godo-Pla et al. 2021). The water-treatment plant in Doha is focused on the design of the transfer function, which is the core of the desalination plant interval modeling. The method has more interval systems, this is the disadvantage of this system (Meena et al. 2022). As stated before, the conventional PID controllers also have some limitations in terms of rising time, settling time, and quality metrics. The aforementioned methods have drawbacks that make the chlorination control system less effective, quality, and low performance. To overcome these issues, this work presents the CDM-PID-based polynomial controller to tune the control parameter with the DCS interfaced conical tank. Here, the pilot plant of DCS interfaced with two conical tanks interacting system.

Presented in this paper are materials and methods with the dynamics of one and two tank systems and CDM-PID tuning methods, which are described in Section 2. The transfer functions at different regions, simulation, and experimental validation in a conical tank using a CDM-PID controller loop inside the DCS system is shown in Section 3 and the conclusion is in Section 4.

1. Materials and methods

1.1. Dynamics of conical tank

This section covers conical tank modeling. The tank in this level procedure is conical in shape, and the level of liquid is maintained at a consistent value. This is accomplished by adjusting the tank's input flow. The control variable is the tank level, while the manipulated variable is tank inflow. Figure 2 shows the conical tank system with a triangular section of the conical tank diagram.

By applying the mass balance equation

$$inflow - outflow = rate\ of\ accumulation$$

$$Fin - Fout = A\frac{dh}{dt} \tag{1}$$

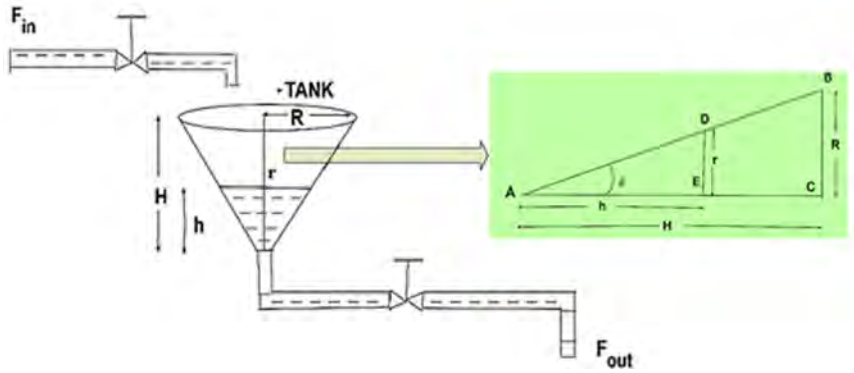

Fig. 2. Conical tank system with a triangular section of the conical tank
F_{out} – Outlet Flow Rate, F_{in} – inlet flow rate, R – top radius of conical tank, H – total height of conical tank, r – radius at water level 'h' of conical tank, h – water-level height in the conical tank

Rys. 2. Stożkowy system zbiornika z trójkątną sekcją stożkowego zbiornika

For the conical tank, the flow rate at the outlet is proportional to the square root of the water level, as shown in Figure 2.

$$Fout \propto \sqrt{h}$$

$$Fout = b\sqrt{h} \tag{2}$$

b is a valve constant

$$Fin - b\sqrt{h} = A\frac{dh}{dt} \tag{3}$$

Consider the triangular section of the conical tank

$$\tan\theta = \frac{Opposite\,side}{Adjacent\,side} = \frac{BC}{AC} = \frac{DE}{AE}$$

$$\frac{R}{H} = \frac{r}{h}$$

$$r = \frac{R}{H}\cdot h$$

$$Area = A = \frac{1}{3}\pi r^2 = \frac{1}{3}\pi\left(\frac{R}{H}\cdot h\right)^2 = \frac{1}{3}\pi\frac{R^2}{H^2}h^2$$

$$Fin - b\sqrt{h} = A\frac{dh}{dt}$$

$$\frac{dh}{dt} = \frac{Fin}{A} - \frac{b\sqrt{h}}{A} \tag{4}$$

$$\frac{dh}{dt} = \frac{Fin}{\frac{1}{3}\pi\frac{R^2}{H^2}h^2} - \frac{b\sqrt{h}}{\frac{1}{3}\pi\frac{R^2}{H^2}h^2}$$

$$\frac{dh}{dt} = \frac{Finh^{-2}}{\frac{1}{3}\pi\frac{R^2}{H^2}} - \frac{bh^{-3/2}}{\frac{1}{3}\pi\frac{R^2}{H^2}}$$

Let

$$\frac{1}{\frac{1}{3}\pi\frac{R^2}{H^2}} = \alpha$$

$$\frac{b}{\frac{1}{3}\pi\frac{R^2}{H^2}} = \beta = b\alpha$$

$$\frac{dh}{dt} = \alpha Finh^{-2} - \beta h^{-3/2}$$

The conical tank is a highly nonlinear model. The two nonlinear functions in the above development of a model are

$$Finh^{-2}$$

$$h^{-3/2}$$

These two nonlinear terms can be linearized by Taylor's series of expansion and the following variables are derived

$$K = \frac{2hs^{1/2}}{b} \tag{5}$$

$$\tau = \frac{2hs^{5/2}}{\beta} \tag{6}$$

1.2. Interacting two-tank conical system

Figure 3 depicts a schematic representation of the proposed two conical tanks in an interaction-type system. A lot of academics have utilized this as a two-tank benchmark problem. The two control valves MV1 and MV2 send the liquid flows from F_{in1} and F_{in2} to tank 1 and tank 2. The fluid in the tanks should be of good quality and firm, and the tank must have a consistent cross-section, but due to the conical tank's depth fluctuation, the discharge in the tank is not straight. The goal of this proposed work is to discover a transfer function of the tank at different heights of the liquid column.

$$f_{in} - f_1 = A_1 \frac{dh_1}{dt} \tag{7}$$

$$f_1 - f_2 = A_2 \frac{dh_2}{dt} \tag{8}$$

$$f_1 = \frac{h_1 - h_2}{R_1} \tag{9a}$$

$$f_2 = \frac{h_2}{R_2} \tag{9b}$$

$$R_1 = K_1 = \frac{2h_{1s}^{1/2}}{b_1}$$

$$R_2 = K_2 = \frac{2h_{2s}^{1/2}}{b_2}$$

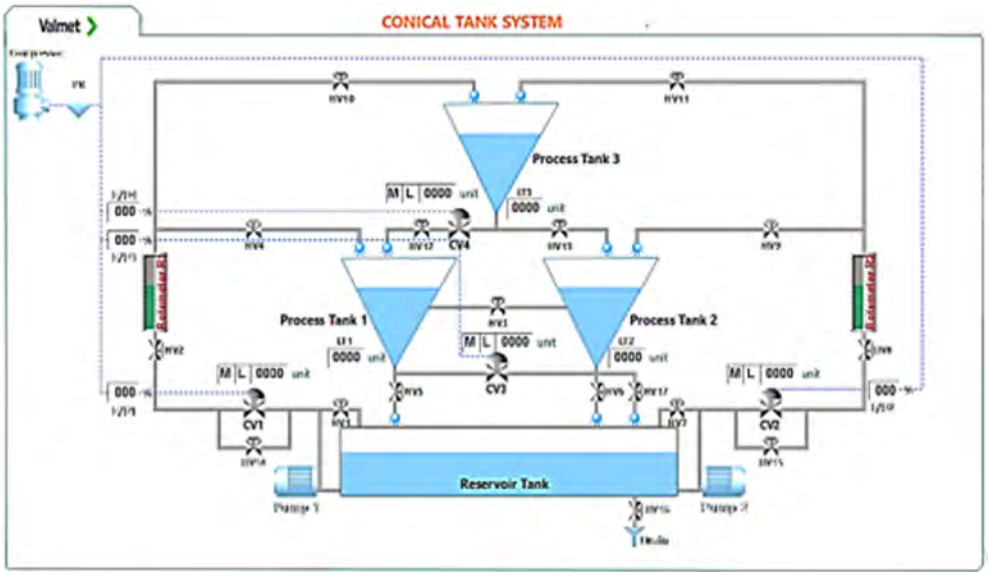

Fig. 3. Proposed two tank interacting conical system

Rys. 3. Proponowane dwa zbiorniki współdziałające z układem stożkowym

A_1 = capacity of the tank $1 = C_1 = \frac{h_{1s}^2}{\alpha_1}$

A_2 = capacity of the tank $2 = C_2 = \frac{h_{2s}^2}{\alpha_2}$

Substitute 9a, 9b in 7 and 8

$$f_{in} - \frac{(h_1 - h_2)}{R_1} = A_1 \frac{dh_1}{dt}$$

$$\frac{(h_1 - h_2)}{R_1} - \frac{h_2}{R_2} = A_2 \frac{dh_2}{dt}$$

$$R_1 f_{in} = A_1 R_1 \frac{dh_1}{dt} + (h_1 - h_2)$$

$$A_2 R_2 \frac{dh_2}{dt} + \left[1 + \frac{R_2}{R_1}\right] h_2 - \frac{R_2}{R_1} h_1 = 0$$

Apply the deviation variables and take Laplace transform;

$$R_1 F_{in}(s) = A_1 R_1 s H_1(s) + H_1(s) - H_2(s) \tag{10}$$

$$A_2 R_2 s H_2(s) + \left[1 + \frac{R_2}{R_1}\right] H_2(s) - \frac{R_2}{R_1} H_1(s) = 0 \tag{11}$$

Where

τ = resistance to the flow X capacity of the tank

$\tau_1 = R_1 A_1 = K_1 C_1$

$\tau_2 = R_2 A_2 = K_2 C_2$

$(1 + s\tau_1) H_1(s) - H_2(s) = R_1 F_{in}(s)$

$$-\frac{R_2}{R_1} H_1(s) + \left(1 + \frac{R_2}{R_1} + s\tau_2\right) H_2(s) = 0$$

Solving the equations give

$$\frac{H_2(s)}{F_{in}(s)} = \frac{K_2}{\left[\tau_1\tau_2 s^2 + \left(\tau_1 + \tau_2 + C_1K_2\right)s + 1\right]} \tag{12}$$

1.3. Coefficient diagram method (CDM)

Even though the CDM appears to be a novel technology, its core ideas have been effectively applied for more than forty-two years in servo control, steel plant motion authority, steam turbine control, and spaceship bow thrusters. With the fundamental principles of CDM, the qualities of classical and modern control capabilities are unified. Polynomial expressions are used by CDM. Because in this formulation, all equations are solved using denominator and numerator polynomials that are independent of one another, better results can be obtained when dealing with cancellation at the pole-zero point. The type and amount of the control polynomial, as well as the closed system's characteristics polynomial, were determined at the start of this technique. The variables of the controller polynomial are then calculated using the design requirements. The "simultaneous approach" is a tactic used by the CDM (Manabe 1998). The concurrent design framework allows the designer to achieve a fair balance between both the rigor of the constraints and the intricacy of the controller. CDM is a capable and rewarding control tool that may be used to plan excellent control systems. Stability, time domain efficiency, and robustness are the requirements of all. A controller is simple and easy to understand to find close relationships. The variables of the polynomial equation are the link between these parameters. As a result, CDM can be used for both control system design and controller tuning. Thus, the smallest controller that satisfies the criteria can be easily realized. The CDM is the mathematical method that produces the most precise results and has the simplest methodology.

1.4. CDM controller design

Figure 4 shows a schematic diagram of a standard feedback control system. The output signal is "y," the reference input is "r," and the disturbance is "d." The controllers and the plant transfer function are denoted by Gc(s) and G(s), respectively.

Gc(s), the controller transfer function shown in Figure 5 is made up of three polynomials. The controller's forward denominator polynomial is A(s) and the feedback numerator polynomials and reference numerator polynomial (Manabe 1998) of the controllers are B(s) and F(s), respectively. Because the operator's transfer function includes two fractions and has a two-degree-of-freedom framework.

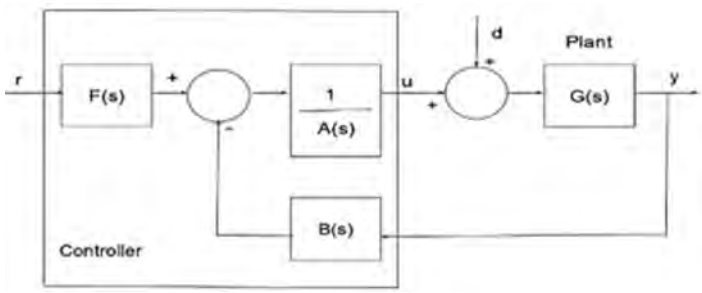

Fig. 4. CDM control system
N(s) – numerator polynomial of the plant, A(s) – forward denominator polynomial, B(s) – feedback numerator polynomial, D(s) – denominator polynomial of the plant, r – input for reference, u – controller output signal, y – output, d – disturbance

Rys. 4. System sterowania CDM

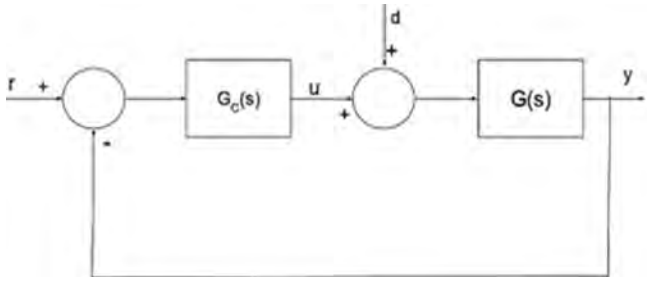

Fig. 5. CDM-based PID control model
N(s) – numerator polynomial of the plant, A(s) – forward denominator polynomial, B(s) – feedback numerator polynomial, D(s) – denominator polynomial of the plant, r – input for reference, u – controller output signal, y – output, d – disturbance

Rys. 5. Model sterowania PID oparty na CDM

To find Y:
For both servo and regulatory control:

$$y = \frac{N(s)F(s)}{A(s)D(s)+N(s)B(s)}r + \frac{N(s)A(s)}{A(s)D(s)+N(s)B(s)} \tag{13}$$

Where

$$P(s) = A(s)D(s)+N(s)B(s) = \sum_{i=0}^{n} a_i s^i, \quad a_i > 0 \tag{14}$$

Where $p \geq q$ should be provided for practical implementation.

According to Manabe, the CDM strategy parameters, time constant

$$\tau = \frac{a_1}{a_0} \tag{15a}$$

Stability indices

$$y_i = \frac{a_i^2}{a_{(i+1)} a_{(i-1)}}, \quad i = 1 \quad to \quad (n-1) \tag{15b}$$

$\gamma_0 = \propto(0)$

Stability limit indices

$$\gamma^*_i = \frac{1}{\gamma_{(i-1)}} + \frac{1}{\gamma_{(i+1)}} \tag{15c}$$

From 15a, 15b and 15c, the coefficients

$$a_i = \frac{\tau_i}{\prod_{j=1}^{(i-1)} \gamma_{i-j}^j} a_0 = z_i a_0 \tag{16}$$

The CDM design parameters are set as follows: comparable integral time (τ).

$\tau = t_s/(2.5 \approx 3)$, where t_s is the user-specified settling time.

The stable indices are usually selected as $\gamma_I = [2.5, 2, 2, \ldots]$.

The target characteristic polynomial is obtained by sub the Equations 15a, 15b, 15c and 16 in Equation 14.

$$P_l(s) = a_0 \left[\left\{ \sum_{i=2}^{n} \left(\prod_{j=1}^{i-1} \frac{1}{\gamma_{i-j}^j} \right) (\tau s)^i \right\} + \tau s + 1 \right] \tag{17}$$

1.5. Controller design for the SOPTD model of interacting two tank conical system

Second Order Plus Time Delay (SOPTD) model of interacting a two-tank conical system is considered for controller design. The two-tank conical system is taken into account in the chlorine scrubber system. The transfer function of the SOPTD model is given in Equation (18).

$$G(s) = \frac{K}{T_1 s^2 + T_2 s + 1} e^{-\theta s} \tag{18}$$

By I order Pada's approximation,

$$e^{-\theta s} = \frac{2 - \theta s}{2 + \theta s} \tag{19}$$

$$G(s) = \frac{-K\theta s + 2K}{T_1 \theta s^3 + (2T_1 + T_2\theta)s^2 + (2T_2 + \theta)s + 2} \tag{20}$$

$N(s) = -K\theta s + 2K$

$D(s) = T_1\theta s^3 + (2T_1 + T_2\theta)s^2 + (2T_2 + \theta)s + 2$

$A(s) = I_1 s$

$B(s) = K_2 s^2 + K_1 s + K_0$

$$P(s) = (I_1 s)\left(T_1\theta s^3 + (2T_1 + T_2\theta)s^2 + (2T_2 + \theta)s + 2\right) + \left(K_2 s^2 + K_1 s + K_0\right)(-K\theta s + 2K) \tag{21}$$

$$P_{Target}(s) = P_t(s) = a_0\left[\left\{\sum_{i=2}^{n}\left(\prod_{j=1}^{i-1}\frac{1}{\gamma_{i-j}^{j}}\right)(\tau s)^i\right\} + \tau s + 1\right] = \tag{22}$$

$$= \frac{\tau^4}{\gamma_1^3\gamma_2^2\gamma_3}s^4 + \frac{\tau^3}{\gamma_1^2\gamma_2}s^3 + \frac{\tau^2}{\gamma_1}s^2 + \tau s + 1$$

Compare Equations 21 and 22, the controller gains are determined

$K_0 = \frac{1}{2K}$; $K_1 = \frac{1}{2K}\left[\tau + KK_0\theta - 2I_1\right]$; $K_2 = \frac{1}{K\theta}\left[\left(2T_1 + T_2\theta\right)I_1 - \frac{\tau^3}{\gamma_1^2\gamma_2}\right]$ and

$$I_1 = \frac{\tau^4}{T_2\theta\gamma_1^3\gamma_2^2\gamma_3}$$

$$K_c = \frac{K_1}{I_1} \tag{23a}$$

$$T_i = \frac{K_0}{I_1} \tag{23b}$$

$$T_d = \frac{K_2}{I_1} \tag{23c}$$

2. Result and discussion

2.1. Experimental setup

Figure 6 demonstrates the real-time implementation of the chlorine scrubber system. In a real-time implementation of a chlorination plant, the emergency chlorine gas scrubber system is designed to safely neutralize unscheduled releases of chlorine in the chlorination building and the chlorine storage area respectively. During operation, 10% NaOH solution is fed into the top of the scrubber column with the help of an Ethylene-Ter-Polymer (ETA) designed distributor to ensure even distribution of the solution over the surface of the packing. As the chlorine comes in contact with the caustic solution, it undergoes a fast-irreversible chemical reaction, so that by the time the gas reaches the top of the column, over 99.5%

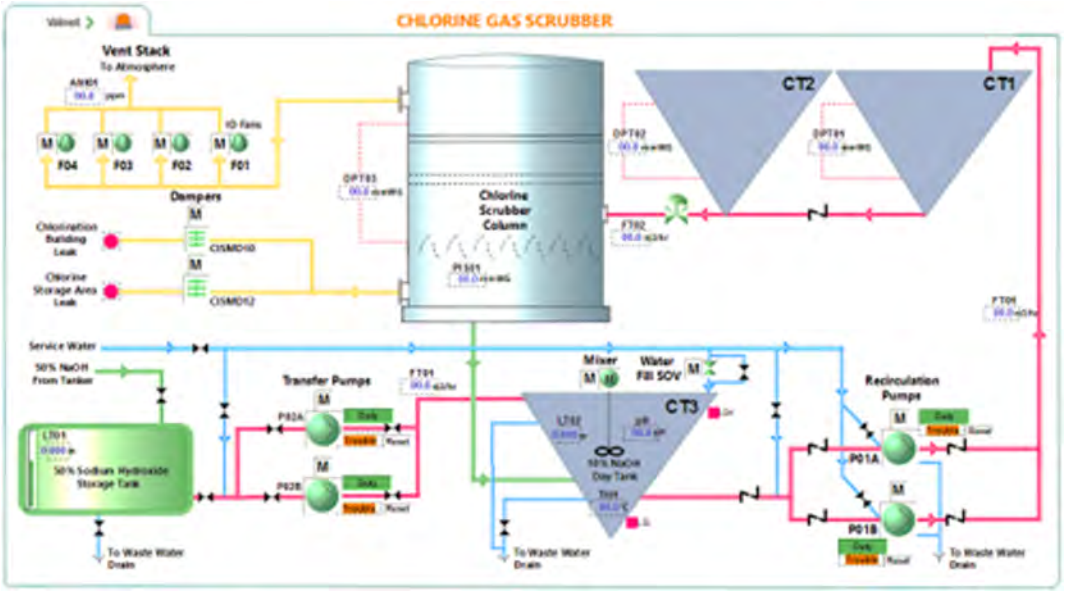

Fig. 6. Real-time chlorine scrubber system

Rys. 6. System płuczki chloru w czasie rzeczywistym

of the chlorine has been removed. A 10% NaOH solution is pumped around the column from a separate day tank. Chlorine gas is drawn through the scrubber column by four induced draft (ID) fans, which are activated by the detection of chlorine leaks in the chlorination building or chlorine storage area. Scrubber operation normally contains a dilution of 50% sodium hydroxide. When a solution of 50% sodium hydroxide at 27°C is diluted to 10% with 27°C water.

The experiment conducted in DCS interacting a two-tank conical system shape of the tank as well as the real-time implementation is the same by comparing the tuning parameters with a different controller. In real-time operation, only the dimension of the conical tank varied.

The experimental setup of the pilot plant of the two-tank conical system is revealed in Figure 7. Tank1 and Tank2 are in an interacting setup, while Tank3 and Tank1 or Tank3 and Tank2 are in a non-interacting setup. Tank1 and Tank2 are considered for further research. The entire Conical tank pilot system is connected to DCS. The experiment is conducted for the input flow of 300 LPH and different valve positions, and the self-regulated steady-state water level is noted. The graph is plotted from the historical data from DCS for the different steady height of water in Tank2.

The tank is non-linear and thus the transfer functions of the interacting system at different regions are derived from the response of the two-tank system to the flow input. The tank is divided into three segments and five regions. The gas scrubber unit operates at the third segment to maintain the pressure for spraying the liquid during scrubbing. Sometimes the liquid height may be in the second segment and thus a single operating region is in the second segment, and the remaining four regions lie in the third segment. The time constants of Tank1 and Tank2 are calculated from the graph with one-point, two-point, and three-point

Fig. 7. Proposed pilot plant DCS interfaced two-tank conical system

Rys. 7. Proponowana instalacja pilotażowa DCS połączona z dwoma zbiornikowymi układami stożkowymi

methods, and the average is taken into consideration. The capacity of the tank is considered from the steady height of the water level and similarly valve resistance. The delay time is noted from the response graph and the obtained transfer function is tabulated. Table 1 illustrates the transfer function with different gains and time constants for the different regions as the system is nonlinear.

Table 1. The transfer function of the interacting two-tank conical system

Tabela 1. Funkcja przenoszenia oddziałującego dwuzbiornikowego układu stożkowego

Region	Transfer function
30–40	$\frac{2.1620}{12,067.4436S^2 + 426.3567S + 1} e^{-30S}$
40–45	$\frac{1.9569}{66,150.713S^2 + 854.2834S + 1} e^{-30S}$
45–50	$\frac{1.5552}{79,781.5672S^2 + 914.7009S + 1} e^{-30S}$
50–55	$\frac{1.5050}{104,861.3075S^2 + 1,019.3519S + 1} e^{-30S}$
55–60	$\frac{1.4562}{148,703.6950S^2 + 1,224.9240S + 1} e^{-30S}$

2.2. Simulation and experimental validation

The selection of control parameters is calculated with different control-tuning methodologies, like Zeigler Nichol's ultimate cycling method, internal model controller, and the coefficient diagram method in MATLAB simulation. The controller tuning parameter is calculated for different regions, as given in Table 2.

The controller gains of the three different tuning methods for five different regions are fed to the Simulink model in MATLAB as well as in the real-time pilot model. The responses of different regions for the real-time pilot model are shown below in Figures 8(a), 8(b), 8(c), 8(d), and 8(e). The performance of the controller, with regard to peak overshoot, settling time, rising time, integral square error (ISE), integral absolute error (IAE), and integral time-weighted absolute error (ITAE) are evaluated and listed in Table 3.

The performance measures of the controller with different tunings are presented in Table 3. To validate the controllers, there are several chances of performance criteria like

Table 2. Controllers tuning parameters

Tabela 2. Parametry strojenia sterowników

ZN-PID			
Region	Kc	Ki	Kd
30–40	4.6288	0.0095	26.1956
40–45	9.4500	0.0067	37.1140
45–50	12.2489	0.0062	40.3091
50–55	14.7106	0.0056	44.9584
55–60	17.3200	0.0050	50.0000
IMC-PID			
30–40	4.2667	0.0103	28.9222
40–45	6.6820	0.0079	78.4421
45–50	8.4047	0.0093	88.3344
50–55	8.7486	0.0087	104.1512
55–60	10.0702	0.0082	121.7553
CDM-PID			
30–40	2.8609	0.0088	57.7098
40–45	3.5328	0.0056	80.7814
45–50	3.8317	0.0047	94.9977
50–55	3.9763	0.0042	102.7762
55–60	3.8348	0.0036	101.3928

attaining a short settling time, maintaining a maximum deviation that is as small as possible, and reducing the integral of errors until the process has settled to its required value, etc. The performance should be measured during dynamic states as well as in the steady state. The integral action in the PID controller can remove offset and thus the steady-state error in the three-mode controller would be zero. The dynamic behavior can be assessed by some characteristic features of the closed-loop system and time-integral performance.

The rise time, overshoot, settling time, and damping factor are commonly used terminology to assess the performance of the controller. The rise time for the ZN-PID is minimum in all the cases and it implies that the control action is quick to reach the desired value. The settling time and peak overshoot are the least in the CDM-PID when compared to other types. The performance of the controller should be fast and robust and is the reasonable trade-off between both. The value of the damping factor assesses both and its value is better in the range 0.50–0.70. The real-time examination gives the damping factor 0.20–0.38, 0.25–0.45,

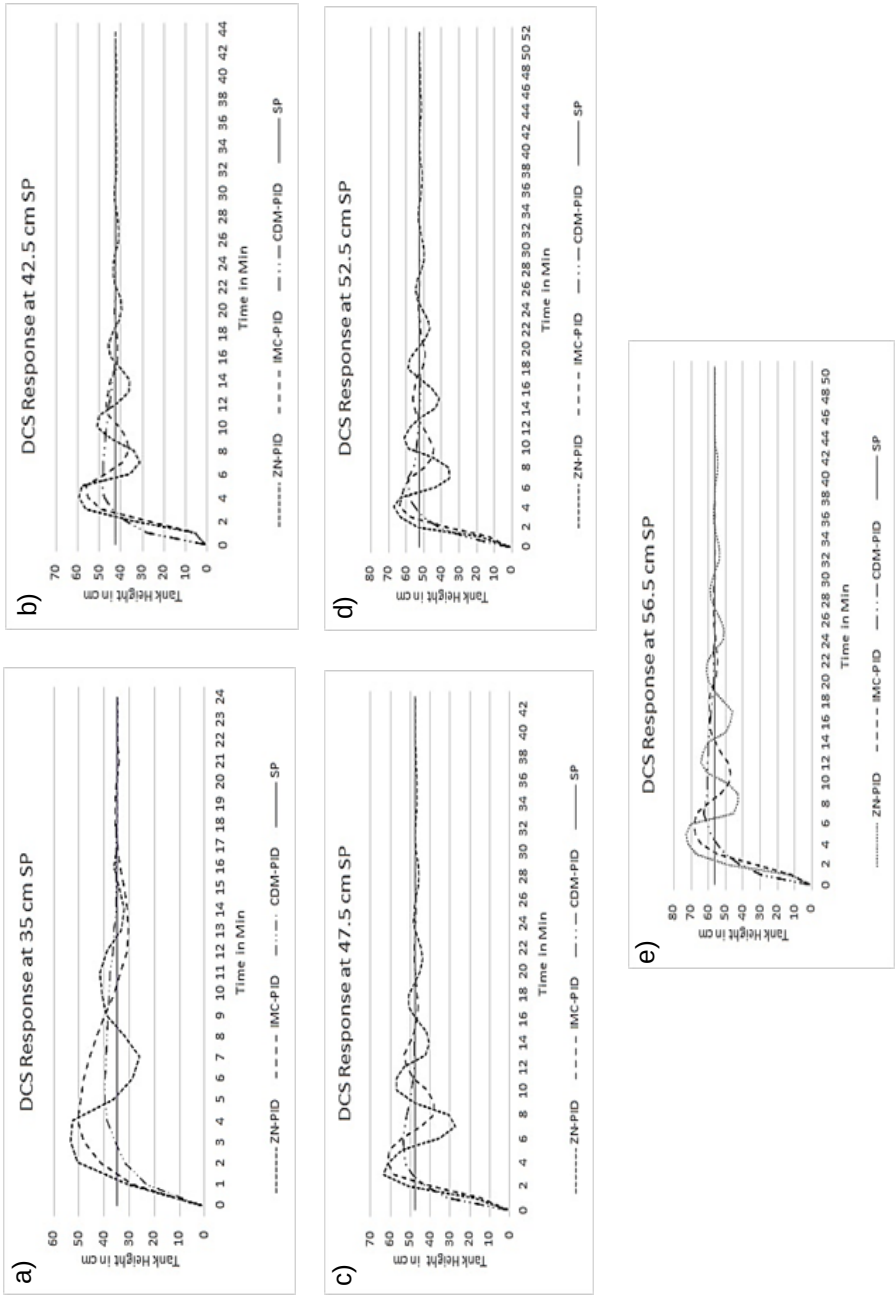

Fig. 8. DCS response at set point (a) 35 cm, (b) 42.5 cm, (c) 47.5 cm, (d) 52.5 cm, (e) 56.5 cm

Rys. 8. Odpowiedź DCS przy wartości zadanej (Setpoint – SP) (a) 35 cm, (b) 42,5 cm, (c) 47,5 cm, (d) 52,5 cm, (e) 56,5 cm

Table 3. Performance measures of the controllers

Tabela 3. Mierniki wydajności kontrolerów

Parameter	ZN PID	IMC PID	CDM PID
Setpoint at 35 cm tank height			
Rise time in min	0.97	1.13	1.87
Settling time in min	17.04	15.76	10.69
Peak overshoot in %	52.49	44.21	13.49
IAE	136.59	148.35	83.17
ISE	2,293.33	2,291.33	1,390.25
ITAE	609.59	759.28	287.55
Setpoint at 42.5 cm tank height			
Rise time in min	1.43	2.05	1.72
Settling time in min	16.32	14.12	12.88
Peak overshoot in %	40.35	31.86	14.02
IAE	213.45	163.78	122.83
ISE	4,330.59	3,791.76	2,353.22
ITAE	1,291.99	606.65	486.19
Setpoint at 47.5 cm tank height			
Rise time in min	1.55	1.93	1.99
Settling time in min	18.37	14.21	9.47
Peak overshoot in %	33.41	28.97	12.55
IAE	233.90	179.12	103.64
ISE	4,727.80	4,093.29	2,578.47
ITAE	1,672.81	771.02	270.39
Setpoint at 52.5 cm tank height			
Rise time in min	1.59	2.23	2.53
Settling time in min	19.78	16.15	8.71
Peak overshoot in %	27.87	21.79	11.82
IAE	277.04	194.00	121.58
ISE	5,597.93	4,912.18	3,480.93
ITAE	2,639.48	909.27	285.44
Setpoint at 56.5 cm tank height			
Rise time in min	1.69	2.41	3.05
Settling time in min	33.07	18.23	15.08
Peak overshoot in %	29.51	20.9	11.44
IAE	315.02	225.91	156.3
ISE	7,054.20	6,364.15	4,191.37
ITAE	2,923.96	1,167.05	646.17

and 0.53–0.57 for ZN-PID, IMC-PID and CDM-PID, respectively. The minimum time integral value of error can be evaluated by the time-integral performance IAE, ISE, and ITAE standards. These strategies depend on the amount and the existence of the deviation. ISE can suppress larger deviations while IAE small errors. ITAE gives more weightage for errors remaining a long time. The investigations of these values give the smallest for CDM-PID in contrast with the other two.

The process can be affected by disturbances, and the controller should overcome the disturbances in minimum time. The disturbance may be due to setpoint change or load, or both. The process is nonlinear and has variable gains and time constants in different regions. The setpoint tracking is difficult and thus regulatory investigation is performed here. A load disturbance is given by the increase in inlet flow rate of about 100 LPH after a steady state is achieved for each region and the response is noted for all controllers. At the 35 cm set point, the disturbance is given at 24 mins for ZN-PID and IMC-PID and 18 mins for CDM-PID. Similarly, at 36, 29, and 20 mins at the 42.5 cm set point; 43, 30, and 19 mins at the 47.5 cm set point; 52, 30, and 19 mins at the 52.5 cm set point; 51, 38, and 26 mins at the 56.5 cm set point for ZN-PID, IMC-PID and CDM-PID, respectively.

Table 4. Regulatory response time

Tabela 4. Regulacyjny czas odpowiedzi

Regulatory Action	ZN PID	IMC PID	CDM PID
35.0 cm SP	22	17	14
42.5 cm SP	29	25	14
47.5 cm SP	30	21	12
52.5 cm SP	34	23	15
56.5 cm SP	37	26	11

Figures 9 to 13 depict the regulatory response of the different controller tunings at several setpoints. The recovery time of the controller to make the tank level reach the desired height in different regions is illustrated in Table 4. The recovery time for ZN-PID, IMC-PID, and CDM-PID is between 22–37, 17–26, and 11–15 minutes, respectively, for different set values. When compared to other tunings like ZN-PID, IMC-PID, and the suggested CMD-PID method, the oscillation will be lower, and the time to reach the steady desired value will be faster. The proposed methodology is more efficient in this case, although all heights vary. In real-time applications, the tuning parameters are compared with different control strategies such as ZN-PID, IMC-PID, and the proposed CDM-PID method. In conclusion, in terms of rising time, settling time, peak overshoot, IAE, ISE, and ITAE, the proposed CDM-PID controller outperforms the existing controllers.

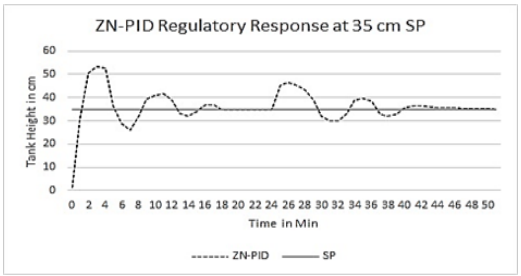

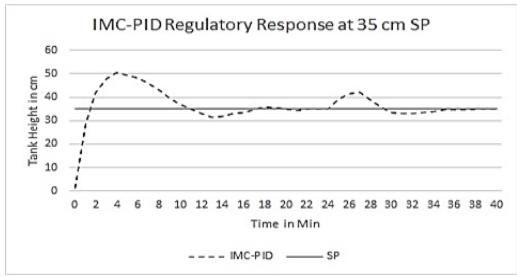

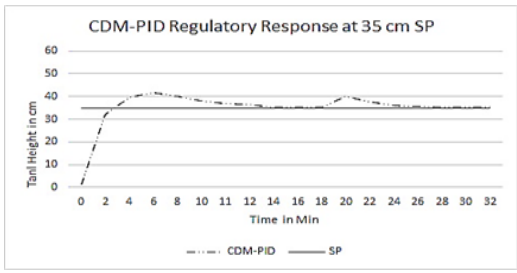

Fig. 9. Disturbance rejection at 35 cm SP for (a) ZN-PID, (b) IMC-PID (c) CDM-PID

Rys. 9. Tłumienie zakłóceń przy wartości zadanej 35 cm SP dla (a) ZN-PID, (b) IMC-PID (c) CDM-PID

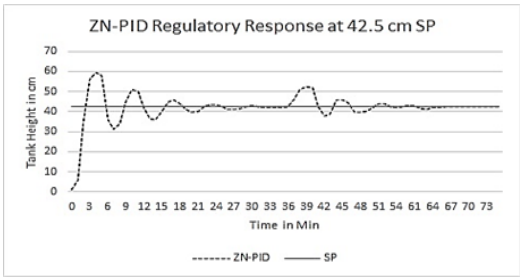

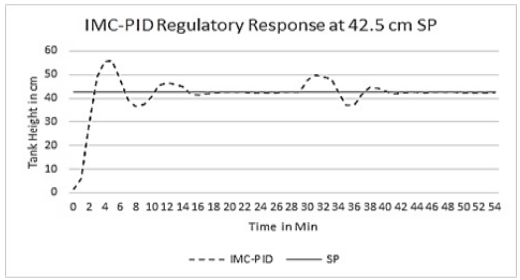

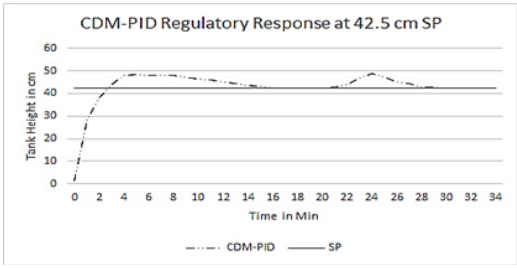

Fig. 10. Disturbance rejection at 42.5 cm SP for (a) ZN-PID, (b) IMC-PID, (c) CDM-PID

Rys. 10. Tłumienie zakłóceń przy wartości zadanej 42,5 cm SP dla (a) ZN-PID, (b) IMC-PID, (c) CDM-PID

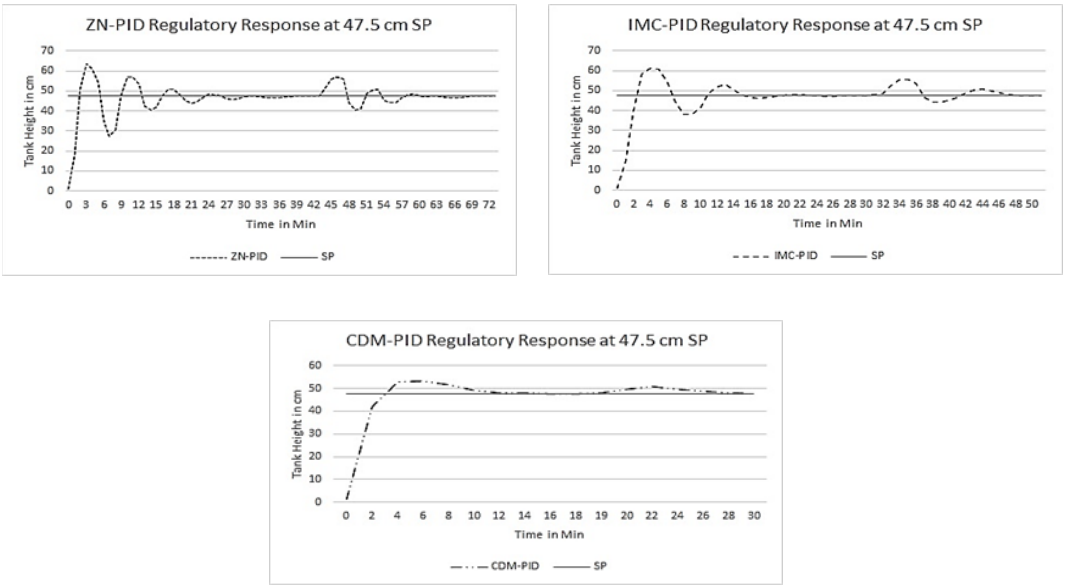

Fig. 11. Disturbance rejection at 47.5 cm SP for (a) ZN-PID (b) IMC-PID, (c) CDM-PID

Rys. 11. Tłumienie zakłóceń przy wartości zadanej 47,5 cm SP dla (a) ZN-PID (b) IMC-PID, (c) CDM-PID

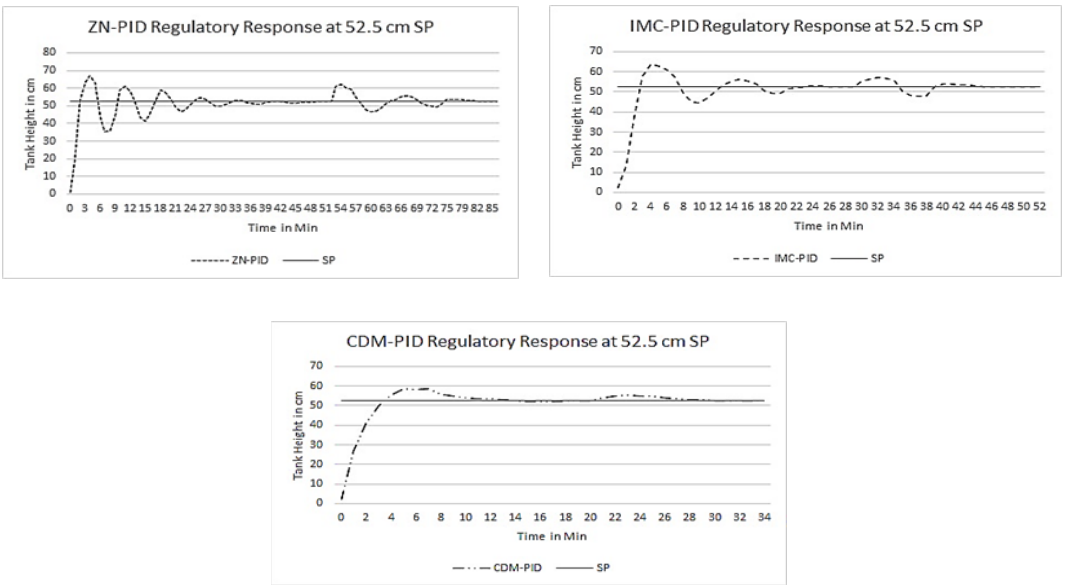

Fig. 12. Disturbance rejection at 52.5 cm SP for (a) ZN-PID, (b) IMC-PID, (c) CDM-PID

Rys. 12. Tłumienie zakłóceń przy wartości zadanej 52,5 cm SP dla (a) ZN-PID, (b) IMC-PID, (c) CDM-PID

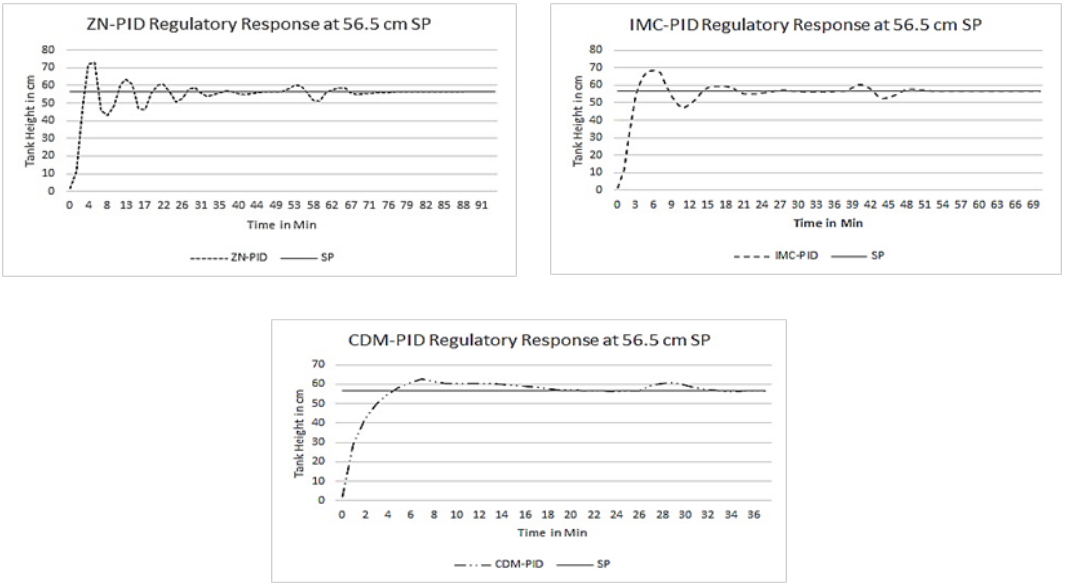

Fig. 13. Disturbance rejection at 56.5 cm SP for (a) ZN-PID, (b) IMC-PID, (c) CDM-PID

Rys. 13. Tłumienie zakłóceń przy wartości zadanej 56,5 cm SP dla (a) ZN-PID, (b) IMC-PID, (c) CDM-PID

Conclusions

In this paper, a CDM-PID control strategy for tuing the control parameter with the DCS interfaced conical tank system is proposed. Instead of the sodium hydroxide tank in the chlorine scrubber system, this work presented the pilot plant of DCS interfaced two conical tanks interacting system with different liquid level heights are evaluated and discussed. Here, the proposed CDM-PID controller tuning strategy is compared with the ZN-PID and IMC-PID controllers. In the proposed system, the CDM-PID controller has less settling time and rise time. The peak overshoot for CDM-PID is the lowest level here and is in the range 9–15%. The damping factor and less overshoot make the system more stable at the same time. The results of IAE, ISE, and ITAE reveal that the proposed CDM-PID method is suitable for all types of deviations. When compared to other tuning ways such as ZN-PID, IMC-PID, and the suggested CDM-PID method, oscillation will be lower, the settling period will be shorter, and the performance lies between speed and robustness, which can eliminate any disturbances in the least time. In real-time applications, the proposed CDM-PID controller also outperformed the existing controllers.

The authors show their sincere gratitude to Peak National General Trading and Contracting Company, w.l.l., Kuwait for providing professional training in DCS and for sharing their rich technical expertise in the field. The authors show their special acknowledgement to the Ministry of Electricity & Water, AlZour South Power station, Kuwait for aiding in identifying the research problem in chlorine gas scrubber systems in chlorination units.

REFERENCES

Asa, E. and Yamamoto, Y. 2021. Aircraft Flight Stabilizer System by CDM Designed Servo State-Feedback Controller. *Aerospace* 8(2), p. 45, DOI: 10.3390/aerospace8020045.

Bhaba, P.K. and Somasundaram, S. 2009. Real time implementation of a new CDM-PI control scheme in a conical tank liquid level maintaining system. *Modern Applied Science* 3(5), pp. 38–45, DOI: 10.5539/mas.v3n5p38.

Coelho et al. 2017 – Coelho, J.P., Pinho, T.M., Boaventura-Cunha, J. and de Oliveira, J.B. 2017. A new brain emotional learning Simulink® toolbox for control systems design. *IFAC-PapersOnLine* 50(1), pp. 16009–16014.

George et al. 2020 – George, M.A., Kamath, D.V. and Thirunavukkarasu, I., 2020, October. An Optimized Fractional-Order PID (FOPID) Controller for a Non-Linear Conical Tank Level Process. [In:] *2020 IEEE Applied Signal Processing Conference (ASPCON)*, pp. 134–138.

Godo-Pla et al. 2021 – Godo-Pla, L., Rodríguez, J.J., Suquet, J., Emiliano, P., Valero, F., Poch, M. and Monclús, H. 2021. Control of primary disinfection in a drinking water treatment plant based on a fuzzy inference system. *Process Safety and Environmental Protection* 145, pp. 63–70, DOI: 10.1016/j.psep.2020.07.037.

Hamamci, S.E. and Tan, N. 2006. Design of PI controllers for achieving time and frequency domain specifications simultaneously. *ISA transactions* 45(4), pp. 529–543, DOI: 10.1016/S0019-0578(07)60230-4.

Hegab, H.M. and Zou, L. 2015. Graphene oxide-assisted membranes: fabrication and potential applications in desalination and water purification. *Journal of Membrane Science* 484, pp. 95–106, DOI: 10.1016/j.memsci.2015.03.011.

Heshmati et al. 2020 – Heshmati, M., Noroozian, R., Jalilzadeh, S. and Shayeghi, H. 2020. Optimal design of CDM controller to frequency control of a realistic power system equipped with storage devices using grasshopper optimization algorithm. *ISA transactions* 97, pp. 202–215, DOI: 10.1016/j.isatra.2019.08.028.

Imal, E. 2009. CDM based controller design for nonlinear heat exchanger process. *Turkish Journal of Electrical Engineering & Computer Sciences* 17(2), pp. 143–161, DOI: 10.3906/elk-0905-45.

Kanagasabai, N. and Jaya, N. 2014. Design of multiloop controller for three tank process using CDM techniques. *International Journal on Soft Computing* 5(2), p. 11, DOI: 10.5121/ijsc.2014.5202.

Kumpanya et al. 2000 – Kumpanya, D., Benjanarasuth, T., Ngamwiwit, J. and Komine, N. 2000. PI controller design with feedforward by CDM for level processes. *2000 TENCON Proceedings. Intelligent Systems and Technologies for the New Millennium (Cat. No. 00CH37119)*, IEEE vol. 2, pp. 65–69, DOI: 10.1109/TENCON.2000.888390.

Lavanya et al. 2013 – Lavanya, M., Aravind, P., Valluvan, M. and Caroline, B.E. 2013. Model based control for interacting and non-interacting level process using labview. *International journal of advanced research in electrical, electronics and instrumentation engineering* 2(7).

Manabe, S. 1998. Coefficient diagram method. *IFAC Proceedings Volumes* 31(21), pp. 211–222, DOI: 10.1016/S1474-6670(17)41080-9.

Manic et al. 2016 – Manic, K.S., Devakumar, S., Vijayan, V. and Rajinikanth, V. 2016. Design of centralized PI controller for interacting conical tank system. *Indian Journal of Science and Technology* 9(12), p. 1–4, DOI: 10.17485/IJST/2016/V9I12/89920.

Meena et al. 2022 – Meena, V.P., Anand, A., Verma, R., Khatri, M., Behera, S. and Singh, V.P. 2022. Interval Modeling of Doha Water Treatment Plant. [In:] *Intelligent Computing Techniques for Smart Energy Systems,* pp. 455–462. Springer, Singapore, DOI: 10.1007/978-981-19-0252-9_41.

Roengruen et al. 2009 – Roengruen, P., Tipsuwanporn, V., Puawade, P. and Numsomran, A. 2009. Smith predictor design by cdm for temperature control system. *World Academy of Science, Engineering and Technology* 35.

Sonehara et al. 2016 – Sonehara, M., Van Toai, N. and Sato, T. 2016. Fundamental study of non-contact water salinity sensor by using electromagnetic means for seawater desalination plants. *IEEE transactions on Magnetics* 52(7), pp. 1–4, DOI: 10.1109/TMAG.2016.2537921.

Tlili et al. 2003 – Tlili, M.M., Manzola, A.S. and Amor, M.B. 2003. Optimization of the preliminary treatment in a desalination plant by reverse osmosis. *Desalination* 156(1–3), pp. 69–78.

Zhou, Y. and Tol, R.S. 2004. Implications of desalination for water resources in China – an economic perspective. *Desalination* 164(3), pp. 225–240, DOI: 10.1016/S0011-9164(04)00191-2.

THE IMPLEMENTATION OF A COEFFICIENT DIAGRAM METHOD BASED POLYNOMIAL CONTROLLER FOR A NON-LINEAR PROCESS WITH A DISTRIBUTED CONTROL SYSTEM IN A CHLORINE SCRUBBER SYSTEM

Keywords

chlorination scrubber system, proportional integral derivative (PID) controller, distributed control system (DCS), coefficient diagram method (CDM), interacting conical tank

Abstract

The seawater desalination process is emerging as a substantial source of fresh water by removing salt and minerals from an infinite supply of seawater effectively. The first stage in a desalination plant is the use of chlorine gas to sterilize the microorganisms in the water. During excess chlorine leakage, an alert is activated, employees are relocated away from the site for a specific period, and dampers will be manually opened. This will cause unsafe working conditions and a waste of time. To overcome this problem, this paper proposes a coefficient diagram method based proportional integral derivative (CDM-PID) control strategy for the tune the control parameter with the distributed control system (DCS) interfaced conical tank. During operation, a 10% NaOH solution is injected into the top of the scrubber column using an ethylene-ter-polymer (ETA) designed distributor to ensure that the solution is evenly distributed across the packing surface. The three control strategies are compared to tune the control parameter with the DCS interfaced conical tank. Instead of the sodium hydroxide tank in the chlorine scrubber system, this work presents the pilot plant of DCS interfaced with two conical tank interacting systems with different liquid level heights. Here, the proposed CDM-PID controller is compared with the standard Ziegler-Nichols (ZN)-ultimate cycling method, and the internal model control (IMC) method. The results demonstrated that the proposed CDM-PID approach is superior to existing approaches in terms of low oscillation, settling period, and high robustness.

IMPLEMENTACJA WIELOMIANOWEGO REGULATORA OPARTEGO NA METODZIE DIAGRAMU WSPÓŁCZYNNIKÓW DLA PROCESU NIELINIOWEGO Z ROZPROSZONYM SYSTEMEM STEROWANIA W SYSTEMIE PŁUCZKI CHLORU

Słowa kluczowe

system oczyszczania chloru, regulator proporcjonalno-całkująco-różniczkujący (PID), rozproszony system sterowania (DCS), metoda diagramu współczynników (CDM), współpracujący zbiornik stożkowy

Streszczenie

Proces odsalania wody morskiej staje się znaczącym źródłem świeżej wody dzięki skutecznemu usuwaniu soli i minerałów z nieskończonych zasobów wody morskiej. Pierwszym etapem w zakładzie odsalania jest użycie chloru gazowego do sterylizacji mikroorganizmów w wodzie. Podczas nadmiernego wycieku chloru zostanie aktywowany alarm, pracownicy zostaną na pewien czas przeniesieni z terenu zakładu, a klapy zostaną ręcznie otwarte. Spowoduje to niebezpieczne warunki pracy i stratę czasu. Aby rozwiązać ten problem, w niniejszym artykule zaproponowano strategię sterowania opartą na metodzie wykresu współczynników proporcjonalno-całkująco-różniczkujących (*Coefficient Diagram Method-Proportional Integral Derivative* – CDM-PID) w celu dostrojenia parametru sterowania za pomocą zbiornika stożkowego połączonego z rozproszonym systemem sterowania (*Distributed Control System* – DCS). Podczas pracy do góry płuczki wstrzykuje się 10% roztwór NaOH za pomocą dystrybutora zaprojektowanego z etylenu-ter-polimeru (*Ethylene-Ter-Polymer* – ETA), aby zapewnić równomierne rozprowadzenie roztworu na powierzchni wypełnienia. Trzy strategie sterowania są porównywane w celu dostrojenia parametru kontrolnego za pomocą zbiornika stożkowego połączonego z DCS. Zamiast zbiornika wodorotlenku sodu w systemie płuczki chloru, w niniejszej pracy przedstawiono Instalację Pilotażową DCS połączoną z dwoma współpracującymi ze sobą stożkowymi układami zbiorników o różnych wysokościach poziomu cieczy. Tutaj, proponowany regulator CDM-PID jest porównywany ze standardową metodą Zieglera-Nicholsa *(ZN)-Ultimate Cycling* oraz metodą kontroli modelu wewnętrznego (*Internal Model Control* – IMC). Wyniki pokazały, że proponowane podejście CDM-PID przewyższa istniejące podejścia pod względem niskich oscylacji, okresu osiadania i wysokiej odporności.